MOLECULAR AND CELLULAR BIOLOGY, Aug. 2006, p. 5994–6004 Vol. 26, No. 16
0270-7306/06/$08.00+0 doi:10.1128/MCB.01630-05

Regulation of p27 Degradation and S-Phase Progression by Ro52 RING Finger Protein

Abdelmajid Sabile,[1]†‡ Andrea Michael Meyer,[1,4]† Christiane Wirbelauer,[2] Daniel Hess,[2] Ulrike Kogel,[3] Martin Scheffner,[3] and Wilhelm Krek[1]*

Institute of Cell Biology, ETH-Hönggerberg, 8093 Zurich, Switzerland[1]; Friedrich Miescher Institute, Maulbeerstrasse 66, 4058 Basel, Switzerland[2]; Department of Biology, University of Konstanz, D-78457 Konstanz, Germany[3]; and Zurich PhD Program in Molecular Life Sciences, Zurich, Switzerland[4]

Received 23 August 2005/Returned for modification 22 September 2005/Accepted 5 June 2006

Ubiquitin-mediated degradation of the cyclin-dependent kinase inhibitor p27 provides a powerful route for enforcing normal progression through the mammalian cell cycle. According to a current model, the ubiquitination of p27 during S-phase progression is mediated by SCF^{Skp2} E3 ligase that captures Thr187-phosphorylated p27 by means of the F-box protein Skp2, which in turn couples the bound substrate via Skp1 to a catalytic core complex composed of Cul1 and the Rbx/Roc RING finger protein. Here we identify Skp2 as a component of an Skp1–cullin–F-box complex that is based on a Cul1-Ro52 RING finger B-box coiled-coil motif family protein catalytic core. Ro52-containing complexes display E3 ligase activity and promote the ubiquitination of Thr187-phosphorylated p27 in a RING-dependent manner in vitro. The knockdown of Ro52 expression in human cells with small interfering RNAs causes the accumulation of p27 and the failure of cells to enter S phase. Importantly, these effects are abrogated by the simultaneous removal of p27. Taken together, these data suggest a key role for Ro52 RING finger protein in the regulation of p27 degradation and S-phase progression in mammalian cells and provide evidence for the existence of a Cul1-based catalytic core that utilizes Ro52 RING protein to promote ubiquitination.

Work over the past decades has delineated many of the key components of the principle pathways that control mammalian G_1 progression, including the D- and E-type cyclins and their associated cyclin-dependent protein kinases (CDKs), CDK4/6 and CDK2, as well as specific polypeptide inhibitors that disrupt cyclin-CDK function (21). One of these CDK inhibitors, p27, has emerged as a central brake to the cell cycle in response to a variety of negative signals. p27 binds to and inhibits the activity of cyclin E-CDK2 complexes and, thus, blocks S-phase progression. The amount of p27 increases in quiescent cells or cells undergoing differentiation. In fact, it is a rate-determining component of cell cycle exit in a number of cell types. Mitogenic stimuli, in turn, liberate cyclin E-CDK2 complexes from p27-mediated inhibitory constraints, thereby allowing quiescent cells to reenter the cell cycle (30).

One major route of p27 inactivation during S-phase entry involves the ubiquitin-proteasome pathway. The polyubiquitination and destruction of p27 is initiated by its phosphorylation on Thr187, which is governed by CDK2 (23). This reaction is thought to earmark p27 for recognition by the Skp1–cullin–F-box (SCF) ubiquitin protein ligase complex SCF^{Skp2} that binds phosphorylated p27 through the F-box protein Skp2 (3, 33, 34) and its cofactor Csk1 (8, 31). A current model holds that Skp2, in turn, links the bound substrate via Skp1 to the Cul1-Rbx1/Roc1 RING finger catalytic core complex (36). Although Skp2 has been implicated in mediating the degradation of multiple key cell cycle regulatory proteins (36), the CDK inhibitor p27 remains the best-characterized substrate of Skp2. In fact, p27 appears to be an essential target of Skp2's S-phase-promoting function. In support of this view, it has been shown that the overexpression of Skp2 promotes p27 degradation (33) and the proliferation defects seen in skp2 knockout mice can be reverted to normal in skp2/p27 double-knockout mice (14, 25). In this regard, low levels of p27 are correlated with poor prognoses in various types of cancer and an inverse relationship between low levels of p27 and high levels of Skp2 in many transformed cells and tumors has been reported (2). Indeed, Skp2 has been shown to act as an oncogene in mouse models and transformation studies (2, 9, 15). Thus, increased Skp2 levels may contribute, at least in part, to abnormally low levels of p27, which are associated with pathological states of excessive cell proliferation, especially cancers.

To further define roles and/or mechanisms of action of Skp2, we sought novel proteins with which Skp2 might interact in the performance of its cell cycle control function. Here we report that Skp2 associates with Ro52, a member of the RING finger B-box coiled-coil (RBCC) motif family of proteins. Ro52 also associates with other SCF components, Skp1 and Cul1, in vivo. The interaction with the latter depends on Cul1 C-terminal sequences previously shown to be required for Rbx/Roc RING finger protein binding, implying that Cul1-Ro52 complexes may represent a new class of catalytic core that serves F-box proteins in ubiquitination reactions. Indeed, Ro52 can also bind the F-box protein βTrCP2. Functional analysis of Ro52 reveals a central role for this RING finger protein in the degradation of Thr187-phosphorylated p27 in vivo and S-phase progression in mammalian cells. Together, our data identify a novel key component of the ubiquitination machinery involved

* Corresponding author. Mailing address: Institute of Cell Biology, ETH-Hönggerberg, 8093 Zurich, Switzerland. Phone: 41 44 633 34 47. Fax: 41 44 633 13 57. E-mail: wilhelm.krek@cell.biol.ethz.ch.

† These authors contributed equally to this work.

‡ Present address: Forschung Orthopaedie, Uniklinik Balgrist, Forchstrasse 340, 8008 Zurich, Switzerland.

in mammalian G_1 cell cycle control and suggest the existence of distinct Skp2-containing E3 ubiquitin ligase complexes that are defined via the molecular nature of the Cul1-RING finger catalytic core.

MATERIALS AND METHODS

Purification of Skp2-associated proteins and mass spectrometric analysis. The purification and identification of Skp2-associated proteins were performed exactly as previously reported (10), except that a mix of Skp2 mouse monoclonal antibodies (MAbs) 60.2, 120.6, and 72.11 was used for immunoprecipitation experiments (33).

Plasmids and siRNAs. pBS-Ro52α plasmid was kindly provided by E. K. L. Chan. To construct pcDNA3-Ro52α and pcDNA3-HA-Ro52α, pBS-Ro52α was used as a template in a PCR to generate an EcoRI/XhoI Ro52α cDNA fragment that was cloned into pcDNA3 or pcDNA3-hemagglutinin (HA) that was previously digested with EcoRI/XhoI. To generate pMalC2-Ro52α, pcDNA3-Ro52α was digested with EcoRI/XbaI and the resulting fragment was cloned into pMalC2 cut with these two enzymes. To construct pcDNA3-Ro52α(ΔR) and pcDNA3-Ro52β, a two-step PCR procedure was employed. The generation of the pcDNA3-MT-Skp2(wt), -(ΔLRR), and -(ΔF30); pcDNA3-MT-Cul1(wt); pcDNA3-Cul1-HA(wt), -(ΔNE), -(ΔBlpI), and -(Δ127); pcDNA3-HA-Cul1(wt); pcDNA3-HA-Cul2(wt); pcDNA3-HA-Cul3(wt); pcDNA3-pVHL(wt); pcDNA3-FT-Skp1; and pcDNA3-FT-Rbx1 constructs has been described previously (17, 18, 37). Ro52α short interfering RNAs (siRNAs), Skp2 siRNAs, and Rbx1 siRNAs were purchased from QIAGEN and correspond to nucleotide sequences 447 to 465 and 914 to 932 in Ro52α, 707 to 725 in Skp2, and 78 to 96 in Rbx1. An additional Rbx1 siRNA (M-004087-1) as well as Cul1 (M-004086-01) and Skp1 (M-003323-2) siRNAs was purchased from Dharmacon. The p27 siRNA was purchased from Santa Cruz (catalog no. sc-29429). An siRNA corresponding to a "scrambled" sequence (QIAGEN) served as a negative control. siRNAs were transfected into subconfluent cells by using Oligofectamine (Invitrogen) according to the manufacturer's instructions.

Antibodies. Antibodies against Skp2, Cul1, and Skp1 have been described previously (18). Anti-p27 (catalog no. sc-528), anti-phospho-p27(Thr187) (catalog no. sc-16324), anti-Cdk2 (catalog no. sc-163), and anti-myc 9E10 antibodies were from Santa Cruz. Monoclonal anti-flag antibody (M2) was from BAbCO. Antitubulin (YL1/2) antibody was from Harlan. The mouse monoclonal antibodies 12CA5 and HA11, recognizing the HA epitope, were purchased from Boehringer Mannheim and BAbCO, respectively. Rabbit polyclonal and mouse monoclonal antibodies recognizing Ro52 were raised against a maltose-binding protein (MBP)-Ro52α fusion protein expressed in bacteria and are referred to as anti-Ro52(fl) and anti-Ro52 MAb 83.34, respectively. The anti-Ro52 MAb was produced in collaboration with AMS Biotechnology Ltd. Polyclonal anti-Rbx1 antibody was raised against human Rbx1 expressed as glutathione *S*-transferase (GST) fusion protein in bacteria. Affinity purification of the different polyclonal rabbit sera was performed as previously described (18).

MBP pull-down assays and in vitro translation. pMal-C2- and pMal-C2-Ro52-transformed bacteria were grown overnight in LB medium supplemented with 100 μg/ml ampicillin. After the induction with 0.1 mM IPTG (isopropyl-β-D-thiogalactopyranoside), bacteria were cultured for an additional 3 h. Bacteria were collected by centrifugation and lysed in NETN buffer (20 mM Tris [pH 8.0], 150 mM NaCl, 1 mM EDTA, 0.5% NP-40, 1 mM phenylmethylsulfonyl fluoride [PMSF], 1 mM dithiothreitol [DTT], 1 μg/ml aprotinin) by sonification. Obtained lysates were centrifuged for 10 min at 10,000 × *g*. Supernatants were incubated with amylose resin (NEB) for 1 h at 4°C. Beads were collected by pulse centrifugation and washed four times in TNN buffer (50 mM Tris [pH 7.5], 250 mM NaCl, 5 mM EDTA, 0.5% NP-40, 50 mM NaF, 0.2 mM Na_3VO_4, 1 mM DTT, 1 mM PMSF, 10 μg/ml aprotinin).

[^{35}S]methionine-labeled in vitro translates of pcDNA3-MT-Skp2(wt) -(ΔLRR), and -(ΔF30); pcDNA3-MT-Cul1(wt); pcDNA3-Cul1-HA(wt), -(ΔNE), -(ΔBlpI), and -(Δ127); pcDNA3-HA-Cul1(wt); pcDNA3-HA-Cul2(wt); pcDNA3-HA-Cul3(wt); pcDNA3-pVHL(wt); pcDNA3-FT-Skp1; pcDNA3/FT-βTrCP1; and pcDNA3/FT-βTrCP2 were produced using a TNT-coupled in vitro transcription translation system (Promega). For MBP pull-down assays, 3 μg of MBP fusion protein bound to amylose beads was incubated with 3 μl of in vitro translates in 500 μl TNN for 1 h at 4°C. Beads were washed four times in TNN buffer, and bound proteins were separated by sodium dodecyl sulfate-polyacrylamide gel electrophoresis (SDS-PAGE). Dried gels were detected by autoradiography.

Cell culture and cell cycle analysis. HeLa and T98G cells were cultivated in Dulbecco's modified Eagle's medium supplemented with 10% fetal calf serum at 37°C in a 10% CO_2-containing atmosphere. For cell synchronization experiments, HeLa cells were arrested in M phase by growth in 250 nM nocodazole for 18 h, washed, and reseeded into fresh, nocodazole-free medium. T98G cells were synchronized in G_0/G_1 by growth in serum-free medium for a period of 72 h and released into the cell cycle by the addition of 20% fetal calf serum. Fluorescence-activated cell sorter (FACS) analysis was performed using a FACSCalibur system (BD Biosciences) as previously described (20). To determine p27 protein stability, we used cycloheximide. Exponentially growing HeLa cells were transfected with siRNAs and then exposed to 20 μg/ml cycloheximide in growth medium. Cells were then incubated at 37°C for different time points and subsequently harvested for immunoblotting.

Immunoprecipitation, immunoblotting, and gel filtration. Immunoprecipitation and immunoblotting experiments were performed exactly as described previously (18). Immunoblots were processed by ECL (Amersham, Piscataway, NJ) according to the manufacturer's instructions. Gel filtration experiments were performed as reported previously (10).

Autoubiquitination and p27 ubiquitination assays. For autoubiquitination, Ro52α was generated in the rabbit reticulocyte lysate system (Promega) in the presence of [^{35}S]methionine. Two microliters of radiolabeled Ro52α was incubated in the presence of 50 ng of recombinant E1, 100 ng of UbcH5, and 20 μg of ubiquitin (Sigma) under standard ubiquitination conditions (11). After incubation at 30°C for 2 h, total reaction mixtures were electrophoresed in 10% SDS-polyacrylamide gels and radiolabeled Ro52α was detected by fluorography. The ubiquitin-activating enzyme E1 and the ubiquitin-conjugating enzyme UbcH5 were expressed in *Escherichia coli* BL21/DE3 as described previously (29).

For in vitro p27 ubiquitination with Ro52 immune complexes, HeLa cell extract prepared from cells transfected with expression plasmids encoding HA-Ro52α, myc-tagged (MT) Skp2, and MT-Cul1 was incubated with anti-HA antibody 12CA5 for 3 h at 4°C. Immune complexes were captured on protein A-Sepharose (30 μl of a 50% slurry) and washed four times with TNN buffer and twice with 1× ubiquitination assay buffer (20 mM HEPES [pH 7.6], 100 mM NaCl, 0.1% Triton X-100, 5 mM $MgCl_2$, 5 mM EDTA, 0.5 mM DTT, 1 mM PMSF, 10 μg/ml aprotinin). The SCF^{Skp2} complex was assembled in Sf9 cells by coinfection with baculoviruses expressing GST-Skp1, Skp2, Cul1, and Rbx1 and captured on glutathione-Sepharose beads as described previously (37). For ubiquitination reactions, a total of 15 μl of washed beads was incubated with 15 μl of in vitro-translated ^{35}S-labeled human p27 that was previously phosphorylated by incubation with cyclin E-Cdk2 complexes bound to GST-$p9^{Cks1}$ in kinase buffer (20 mM HEPES [pH 7.4], 2 mM ATP, 10 mM $MgCl_2$, 1 mM DTT) at 30°C for 45 min. Cyclin E and Cdk2 were produced in Sf9 cells after coinfection with the relevant baculoviruses, and GST-$p9^{Cks1}$ was isolated from bacteria. Ubiquitination reactions in a total volume of 30 μl contained 3 μl 10× ATP-regenerating system (20 mM HEPES [pH 7.2], 10 mM ATP, 10 mM magnesium acetate, 300 mM creatine phosphate, 0.5 mg/ml creatine kinase), 3 μl 10× reaction buffer (40 mM magnesium acetate, 5 mM DTT, 1 mM PMSF), 10 μg ubiquitin, 2 μM ubiquitin aldehyde, 0.6 μg E1, 2 μg CDC34 or UbcH5, and 2 μM MG132 (Sigma). Reaction volumes were adjusted to 30 μl with 1× ubiquitination assay buffer. Reactions were carried out at 30°C for 120 min and stopped with 3× SDS sample buffer. The products were analyzed by SDS-PAGE followed by autoradiography.

RESULTS

Identification of Ro52 as a Skp2-associated protein. In search of novel Skp2-associated proteins using mass spectrometry, we identified Ro52 (Fig. 1A), a member of the RBCC family and a major target of autoantibodies in autoimmune conditions such as systemic lupus erythematosus and Sjögren's syndrome (5, 27). The full-length Ro52 protein is comprised of three distinct domains: an N-terminal RING–B-box motif, a central coiled-coil domain, and C-terminal PRY and SPRY domains. Ro52 has been reported to exist in two forms, Ro52α and a splice variant, Ro52β, which lacks the central coiled-coil domain. The latter variant appears to be highly expressed in the fetal stages of various organs (4). Ro52 mRNAs are inducible by gamma interferon (28), and its protein product has also been implicated in CD28-mediated interleukin-2 production (12). Interestingly, Ro52 contains distinct signature motifs that constitute a RING

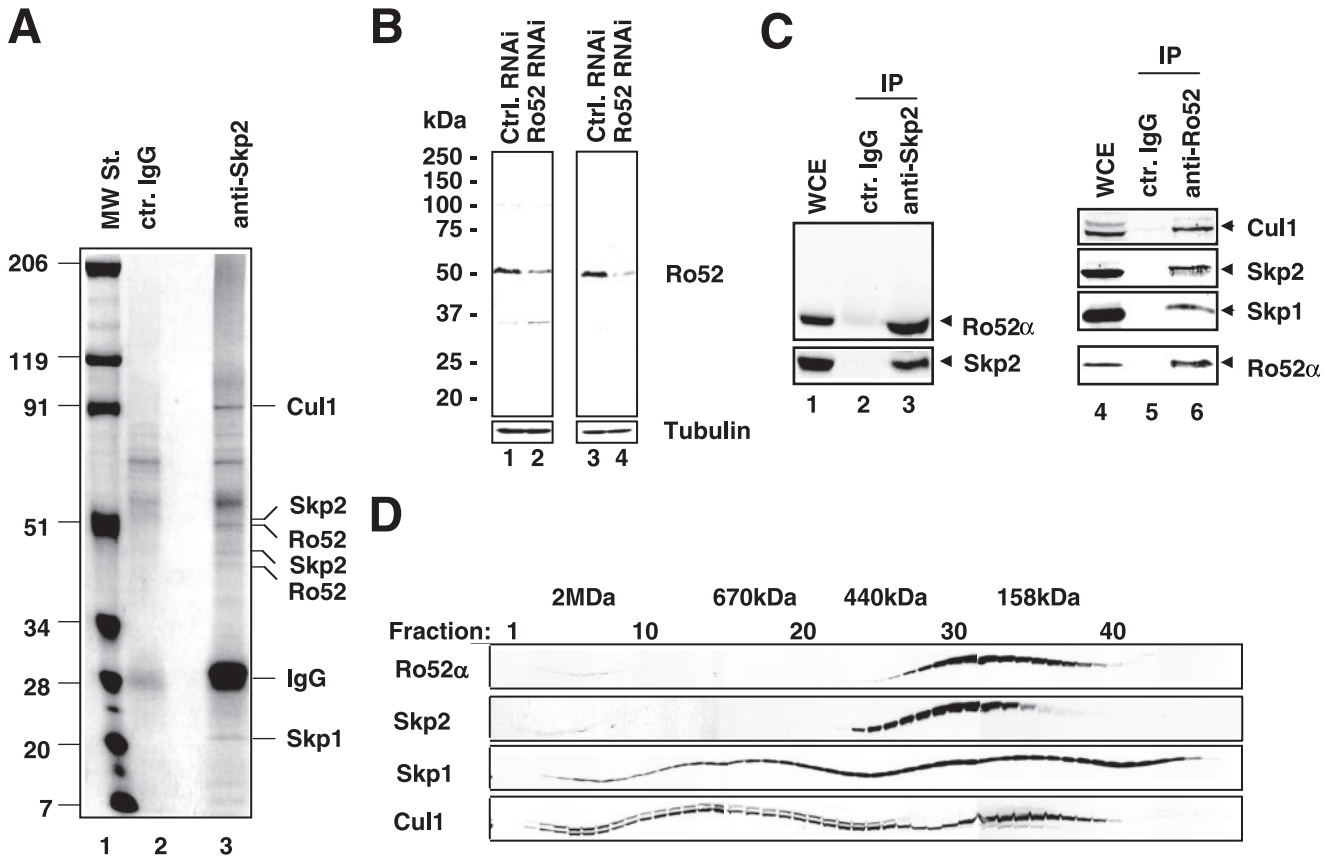

FIG. 1. Isolation of Ro52 as a Skp2-associated protein. (A) Immunoprecipitates from HeLa cell extracts with control (ctr.) mouse IgG (lane 2) or a mix of Skp2 mouse MAbs 60.2, 120.6, and 72.11 (lane 3). Polypeptides that yielded unambiguous mass spectrometry spectra are indicated. MW St., molecular weight standard. (B) Characterization of Ro52 polyclonal and monoclonal antibodies. HeLa cells were transfected with either control (ctrl.) or Ro52 siRNAs, and whole-cell extracts were processed for immunoblotting with affinity-purified anti-Ro52(fl) polyclonal (lanes 1 and 2) or anti-Ro52(83.34) monoclonal (lanes 3 and 4) antibodies and membranes were reblotted for the expression of tubulin. (C) Aliquots of whole-cell extracts (WCE) of HeLa cells were subjected to immunoprecipitation (IP) with control (ctr.) mouse IgG (lanes 2 and 5) or either anti-Skp2 MAb mix 60.2, 120.6, and 72.11 (lane 3) or anti-Ro52 MAb 83.34 (lane 6), and the immunoblot was probed with anti-Ro52(fl) and anti-Skp2(fl) (lanes 2 and 3) and anti-Ro52(fl), anti-Skp1 MAb mix 96.20 and 57.2, and anti-Skp2 MAb mix and anti-Cul1(ct) (lanes 5 and 6). Other aliquots were directly processed for immunoblotting by using the above-noted antibodies (lanes 1 and 4). (D) Gel filtration analysis. A whole-cell lysate of HeLa cells was fractionated on a Superose 6 gel filtration column, and individual fractions were processed for Western blotting using antibodies to the indicated proteins.

finger domain and that have been implicated in the ubiquitination process (19). RING domains are a common feature of many E3 ubiquitin ligases (6). In this regard, Ro52 is itself mono- and polyubiquitinated, although the significance of that modification remains elusive (7). These observations, combined with the fact that Ro52 is present in Skp2 immunoprecipitates (Fig. 1A), license the speculation that at least one potential biochemical function of Ro52 might be directly linked to its role as E3 component in conjunction with Skp2.

To study this possibility further, we raised Ro52-specific polyclonal and monoclonal antibodies. Affinity-purified anti-Ro52(fl) polyclonal and anti-Ro52(83.34) monoclonal antibodies detected a single prominent band of 52 kDa in whole-cell extracts of HeLa cells (Fig. 1B, lanes 1 and 3, respectively). This band was significantly downregulated in cell extracts derived from Ro52 siRNA-treated HeLa cells (Fig. 1B, lanes 2 and 4), indicating that these antibodies recognize bona fide Ro52. Although Skp2 eluates used for mass spectrometric identification of Skp2-associated proteins also contained a smaller form of Ro52 (see Fig. 1A), we note that this form represents a degradation product of the larger form of Ro52, Ro52α, and not Ro52β, as the latter is not expressed at detectable levels in HeLa, HEK293, or T98G cells.

Skp2 MAb immunoprecipitates contained endogenous Ro52α, confirming the above-noted finding (Fig. 1C, lane 3). Ro52α was not detected in immunoprecipitates with control mouse immunoglobulin G (IgG) (lane 2). In reciprocal immunoprecipitates, Skp2 was present in Ro52 MAb (Fig. 1C, lane 6) but not in control IgG (lane 5) immunoprecipitates. In addition, endogenous Skp1 and Cul1 coimmunoprecipitated specifically with Ro52 (Fig. 1C, lane 6). In accord with these findings, Ro52α also eluted closely together with Skp2 on gel filtration (Fig. 1D). Taken together, these results suggest that Ro52α associates with core components of SCF^{Skp2}, in particular, Skp2, Skp1, and Cul1 in vivo. The finding that part of endogenous Ro52 localizes to the nucleus (data not shown) is consistent with a physical interaction of Skp2, Skp1, and Cul1 with Ro52 in vivo.

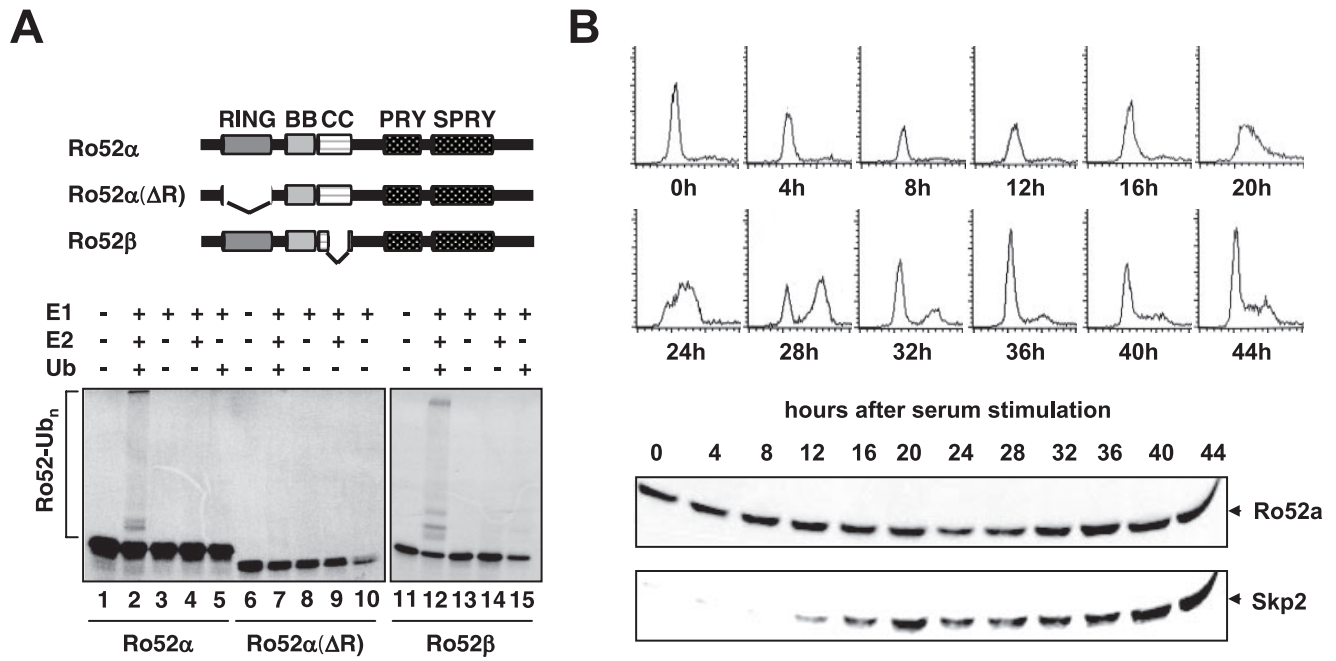

FIG. 2. Ro52 displays autoubiquitination activity. (A) Autoubiquitination of Ro52. Upper panel, schematic of Ro52 species used in the analysis. Autoradiograms of ^{35}S-labeled Ro52α, Ro52α(ΔR), and Ro52β after in vitro autoubiquitination. −, presence of; +, absence of. (B) T98G cells were arrested in G_0/G_1 by serum deprivation and stimulated to reenter the cell cycle by the addition of serum. At the indicated times thereafter, whole-cell extracts were prepared, equalized for protein content, and processed for immunoblotting using antibodies against the indicated proteins (lower panel). In parallel, aliquots of cells were processed for FACS analysis to determine cell cycle distribution (upper panel).

Ro52 displays RING-dependent E3 ligase activity in vitro. There is ample evidence that RING finger proteins mediate protein ubiquitination in the presence of certain E2 ubiquitin-conjugating enzymes. Furthermore, a common feature of many RING finger E3s is their ability to ubiquitinate themselves ("autoubiquitination"). Therefore, we asked whether Ro52α or -β displays autoubiquitination activity in vitro and, if so, whether such activity is dependent on the presence of an intact Ro52 RING finger domain. As shown in Fig. 2A, ^{35}S-labeled, in vitro-translated Ro52α or -β was autoubiquitinated in vitro in the presence of ubiquitin, E1, and the E2 enzyme UbcH5, as indicated by the appearance of a high-molecular-weight smear that is characteristic of ubiquitin conjugates (lanes 2 and 12). No such ubiquitination activity was detected with Ro52α(ΔR), a mutant lacking the RING finger domain (Fig. 2A, lane 7), or when UbcH5 was replaced with the E2 enzyme CDC34 (data not shown). These results establish that both Ro52α and -β have the capacity to function as E3 ligases. Since Ro52α protein levels do not fluctuate during cell cycle progression (Fig. 2B), a functional association of Ro52α with Skp2 is expected to develop in late G_1 and S phases, times when Skp2 expression is induced (Fig. 2B).

Ro52 interacts with Skp2 and βTrCP2. Next we assessed the structural requirements for Ro52-Skp2 complex formation. MT-Skp2 and HA-tagged Ro52α(wt) (where wt is wild type) or HA-Ro52α(ΔR) were transiently transfected, individually or together, into HeLa cells. A HA MAb, 12CA5, coimmunoprecipitated MT-Skp2 from cells cotransfected with both expression vectors but not from cells transfected with MT-Skp2 alone (Fig. 3A, lane 4). MT-Skp2 also coimmunoprecipitated with HA-Ro52α(ΔR), which lacks the RING finger domain (Fig. 3B, lane 4). Hence, Ro52 interacts with Skp2 in a RING finger-independent manner.

To test whether Ro52 can also interact with other F-box proteins or close relatives, in vitro-translated, flag-tagged (FT) βTrCP1, βTrCP2, or pVHL was incubated with MBP-Ro52 fusion proteins. While βTrCP2 bound efficiently to MBP-Ro52 (Fig. 3C, lane 6), βTrCP1 bound poorly and pVHL did not bind at all (Fig. 3C, lanes 4 and 8, respectively). Similarly, after transient transfection of FT-βTrCP2 and HA-Ro52α into HeLa cells, FT-βTrCP2 was detected in Ro52 MAb 83.34 immunoprecipitates (Fig. 3D, lane 6), while FT-βTrCP1 was not detectable (Fig. 3D, lane 4). Thus, Ro52 can interact with at least one other F-box protein in vitro and in vivo, raising the possibility that it can functionally associate with distinct F-box proteins.

Interestingly, Ro52 binding to the F-box protein Skp2 did not depend on an intact F-box, since in vitro-translated MT-Skp2(ΔF30), an F-box deletion mutant defective for Skp1 binding, was still able to bind to MBP-Ro52 in a manner similar to that of the wild-type protein (Fig. 3E, lanes 4 and 8). In contrast, MT-Skp2(ΔLRR), a mutant lacking the leucine-rich domain, failed to bind to MBP-Ro52 in this assay (Fig. 3E, compare lanes 6 and 7). Although the Skp2-Ro52 complex formation appears to be F-box domain independent, we found that Skp1 is required for the efficient interaction of Ro52-Skp2 in vivo, as evidenced by the fact that a knockdown of Skp1 by siRNA significantly reduced the amounts of Skp2 in Ro52 immunoprecipitates without affecting the overall levels of Skp2 and Cul1 (Fig. 3F, lane 3). Thus, Skp1 contributes to efficient Ro52-Skp2 complex formation in vivo.

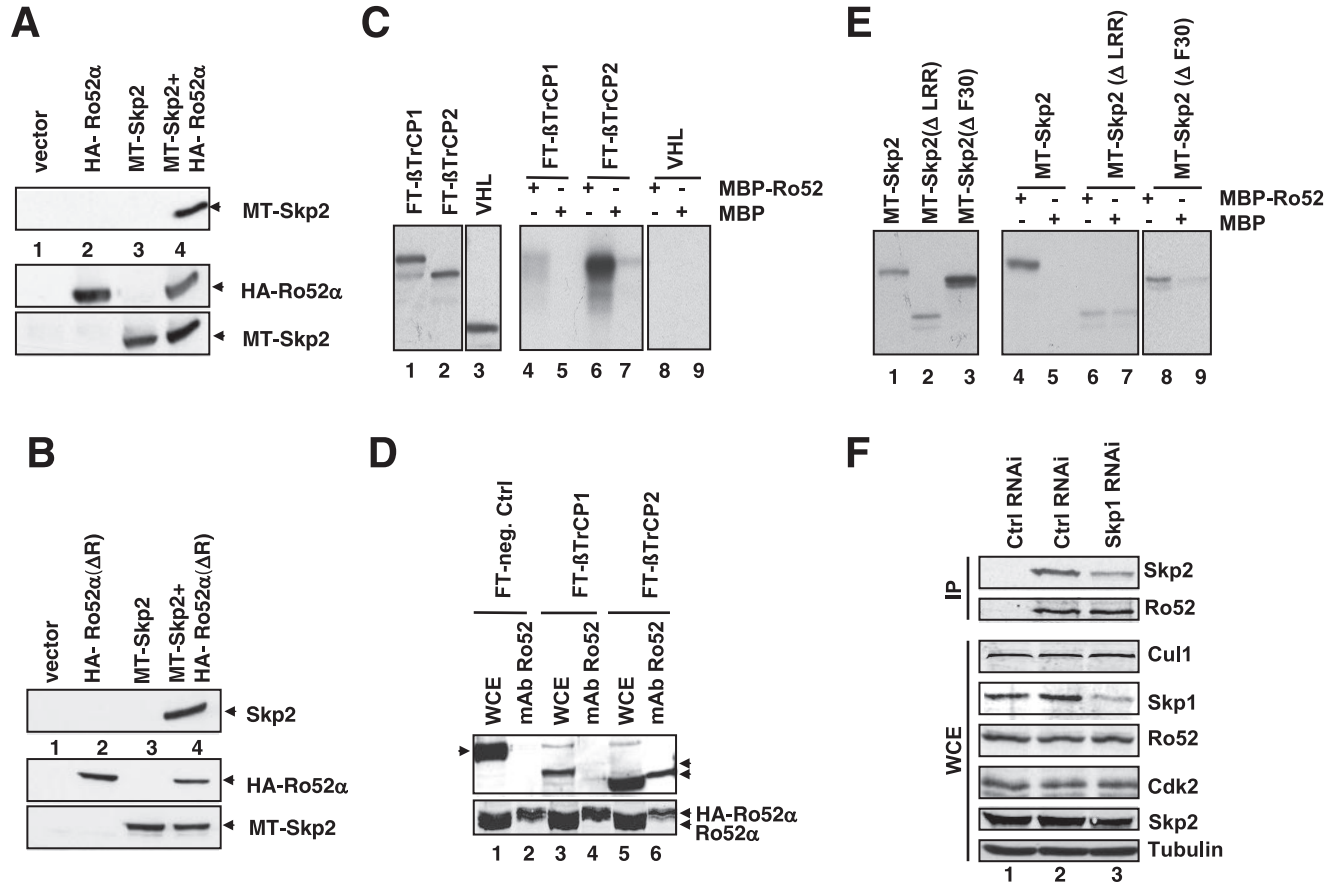

FIG. 3. Ro52α interacts with Skp2 and βTrCP. (A) HA-Ro52α and MT-Skp2 were expressed individually or together in HeLa cells, and aliquots of lysates were either subjected to immunoprecipitation with anti-HA 12CA5 antibody followed by immunoblotting with rabbit anti-Skp2(fl) antibody (upper panel) or directly processed for immunoblotting with anti-HA MAb HA11 (middle panel) or anti-Myc MAb 9E10 (lower panel). (B) The panel shown is as described for panel A, except that HA-Ro52α(ΔR) lacking the RING domain was transfected instead of HA-Ro52α(wt). (C) In vitro translates (IVTs) of FT-βTrCP1, FT-βTrCP2, or pVHL were incubated with MBP (lanes 5, 7, and 9) or MBP-Ro52 (lanes 4, 6, and 8) fusion proteins, and bound proteins were analyzed by SDS-PAGE (lanes 2 through 4). Lanes 1 to 3, input IVTs. −, presence of; +, absence of. (D) FT-mPIAS3L, FT-βTrCP1, or FT-βTrCP2 was expressed in HeLa cells, together with HA-Ro52α, and aliquots were subjected to immunoprecipitation with anti-Ro52 MAb and processed for immunoblotting with anti-FT antibody M2 (upper panel) or anti-Ro52 MAb (lower panel). Other aliquots were directly processed for immunoblotting (whole-cell extracts [WCE]) using anti-Ro52 and anti-FT M2 MAbs. The left arrowhead indicates the migration of FT-mPIAS3L (negative control), while the right arrowheads indicate the positions of FT-βTrCP1 and FT-βTrCP2. (E) IVTs of MT-Skp2, MT-Skp2(ΔLRR), or MT-Skp2(ΔF30) were incubated with MBP (lanes 5, 7, and 9) or MBP-Ro52 (lanes 4, 6, and 8) fusion proteins, and bound proteins were analyzed by SDS-PAGE (lanes 2 to 4). Lanes 1 through 3, input IVTs. (F) HeLa cells were transfected with siRNAs corresponding to either a nonrelevant mRNA (control [ctrl]) (lanes 1 and 2) or Skp1 mRNA (lane 3). Aliquots were processed for immunoprecipitation with either control IgG (lane 1) or anti-Ro52 MAb (lanes 2 and 3) that had been covalently coupled to protein A-Sepharose beads using dimethylpimelimidate and processed for immunoblotting using anti-Skp2 MAb mix or anti-Ro52 MAb 83.34. Other aliquots were directly processed for immunoblotting with antibodies directed against indicated proteins.

Ro52/Cul1 interactions require the cullin homology domain. To study Ro52-Cul1 interactions further, MT-Cul1 and HA-Ro52α(wt) or a HA-Ro52α(ΔR) mutant that lacks the RING finger domain were transiently transfected, individually or together, into HeLa cells. MT-Cul1 coimmunoprecipitated with HA-Ro52α(wt) and with HA-Ro52α(ΔR) from extracts of MT-Cul1 and HA-Ro52α(wt) transfected cells (Fig. 4A and B). Thus, Ro52-Cul1 interactions in vivo, like Ro52-Skp2 interactions, are RING finger independent.

Consistent with the aforementioned results, MBP-Ro52 bound efficiently to in vitro-translated HA-Cul1 (Fig. 4C, lane 4). It did not bind HA-Cul2 or HA-Cul3 (Fig. 4C, lanes 6 and 8, respectively). Next, we analyzed various deletion mutants of Cul1 for Ro52 binding. In particular, we tested Cul1-HA(Δ127), a mutant deleted for the cullin homology domain (residues 452 to 603) and thus deficient for Rbx/Roc binding but still capable of Skp1 binding, Cul1-HA(ΔNE), a mutant that lacks the N-terminal 250 amino acid residues and is deficient for Skp1 binding but proficient for Rbx/Roc binding, and Cul1-HA(ΔBlpI), a mutant lacking the C-terminal 247 amino acid residues and thus defective in Rbx/Roc binding but able to bind to Skp1 (37). As shown in Fig. 4D, the binding of Ro52 to Cul1 is dependent on the same region (spanning residues 452 to 603) of Cul1 that had been previously implicated in Rbx/Roc binding (lane 7). In addition, like Rbx/Roc, Ro52 bound Cul1-HA(ΔNE) (lane 9) but failed to bind to Cul1-HA(ΔBlpI) (lane 11). These results suggest that the requirements for Ro52-Cul1 complex formation are similar to those for Cul1-Rbx/Roc

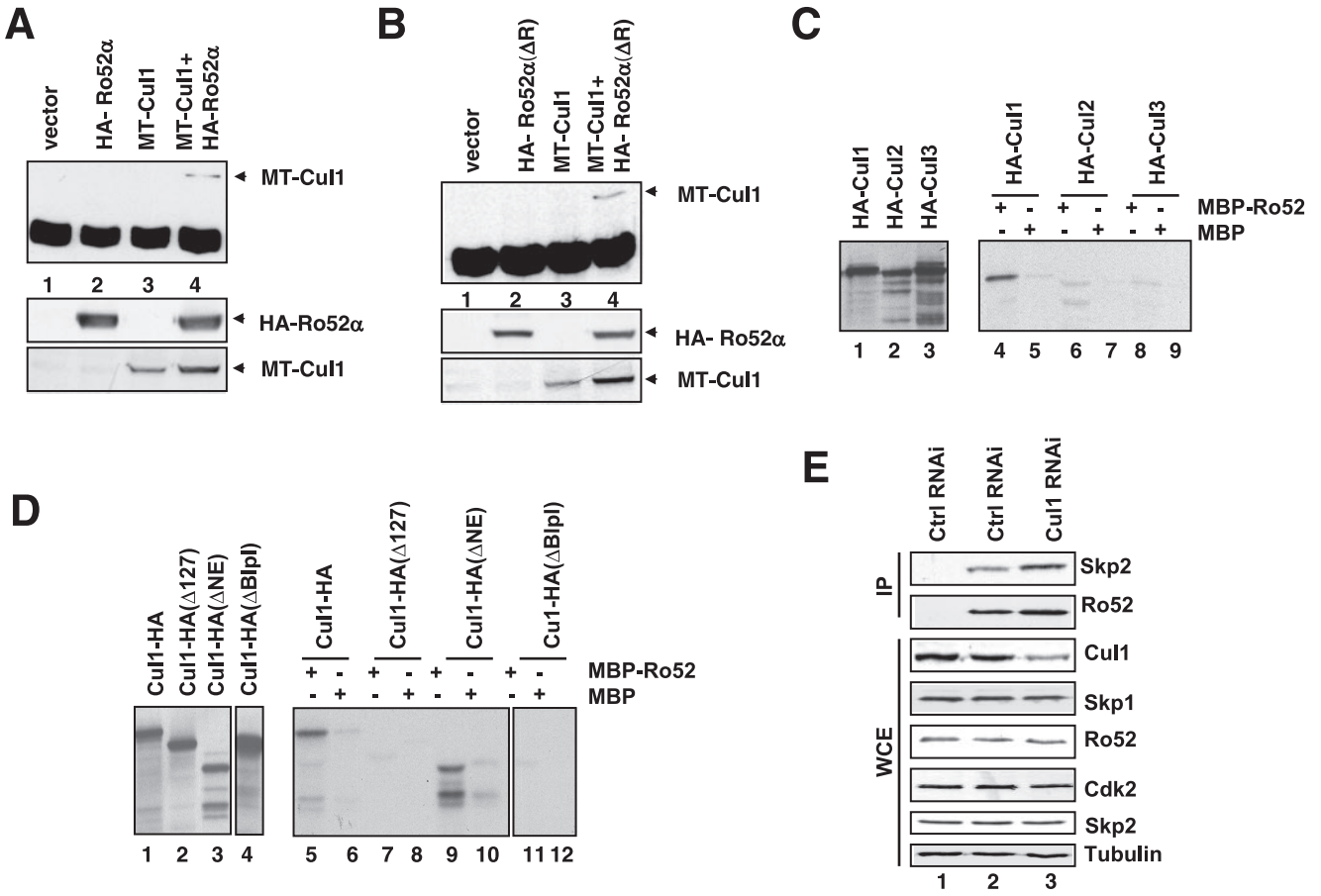

FIG. 4. Cul1 interacts with Ro52 via the cullin homology domain. (A) HA-Ro52α and MT-Cul1 were expressed individually or together in HeLa cells, and aliquots of lysates were either subjected to immunoprecipitation with anti-HA 12CA5 antibody, followed by immunoblotting with rabbit anti-Cul1 antibody (upper panel), or directly processed for immunoblotting with anti-HA MAb HA11 (middle panel) or anti-Myc MAb 9E10 (lower panel). (B) The panel shown is as described for panel A, except that HA-Ro52α(ΔR) lacking the RING domain was transfected instead of HA-Ro52α(wt). (C) IVTs of HA-Cul1, HA-Cul2, or HA-Cul3 were incubated with MBP (lanes 5, 7, and 9) or MBP-Ro52 (lanes 4, 6, and 8) fusion proteins, and bound proteins were analyzed by SDS-PAGE (lanes 2 through 4). Lanes 1 to 3, input IVTs. −, presence of; +, absence of. (D) IVTs of Cul1-HA, Cul1-HA(Δ127), Cul1-HA(ΔNE), or Cul1-HA(ΔBlpI) were incubated with MBP (lanes 6, 8, 10, and 12) or MBP-Ro52 (lanes 5, 7, 9, and 11) fusion proteins, and bound proteins were analyzed by SDS-PAGE (lanes 2 through 4). Lanes 1 to 4, input IVTs. −, presence of; +, absence of. (E) HeLa cells were transfected with siRNAs corresponding to either nonrelevant mRNA (control; lanes 1 and 2), or Cul1 mRNA (lane 3). Aliquots were processed for immunoprecipitation (IP) with either control IgG (lane 1) or anti-Ro52 MAb (lanes 2 and 3) that had been covalently coupled to protein A-Sepharose beads using dimethylpimelimidate and processed for immunoblotting using anti-Skp2 MAb mix or anti-Ro52 MAb 83.34. Other aliquots were directly processed for immunoblotting with antibodies directed against indicated proteins. WCE, whole-cell extracts.

interactions. Thus, Ro52 may occupy, in the context of Cul1 complexes, a role analogous to that of Rbx/Roc. Finally, in contrast to Skp1, diminishing Cul1 protein by siRNA did not affect Ro52-Skp2 complex formation (Fig. 4E, compare lanes 2 and 3).

Ro52 participates in the ubiquitination and degradation of Thr187-phosphorylated p27. The facts that Skp2 has emerged as a central regulator of p27 degradation (3, 14, 24, 25, 33, 34) and Ro52α forms complexes with Skp2, Skp1, and Cul1 in vivo raise the question of whether Ro52α participates in a p27 degradation process in vivo. To this end, we monitored p27 levels after experimental reduction of Ro52 protein using different siRNAs. For control, we also silenced Skp2 expression in parallel. Exponentially growing HeLa cells transfected with siRNAs targeting either Skp2 or Ro52 displayed a dramatic increase in the steady-state levels and half-life of p27 compared with that of control siRNA (Fig. 5A and B, respectively). No such changes in protein levels were detected for SCF^{Skp2} components Cul1, Skp1, and Rbx1/Roc1 (Fig. 5A) or Cdk2 (Fig. 5A and B). These results establish an intimate link between the presence of Ro52 protein and the efficient suppression of p27 stabilization and accumulation in vivo.

The degradation of p27 by the ubiquitin-proteasome pathway occurs by Skp2 recognition of a p27 form that is specifically phosphorylated on threonine 187 (Thr187). The immunoblotting of HeLa cell lysates, derived from cells depleted for Skp2 or Ro52 by siRNA, with a p27 phospho-(Thr187)-specific antibody revealed a marked increase of the Thr187-phosphorylated form of p27 (Fig. 5C, lanes 2 and 3). No increase of this modified form of p27 was seen in the cell lysates derived from cells transfected with control siRNA (lane 1). These results identify Ro52 as a key component of the machinery that de-

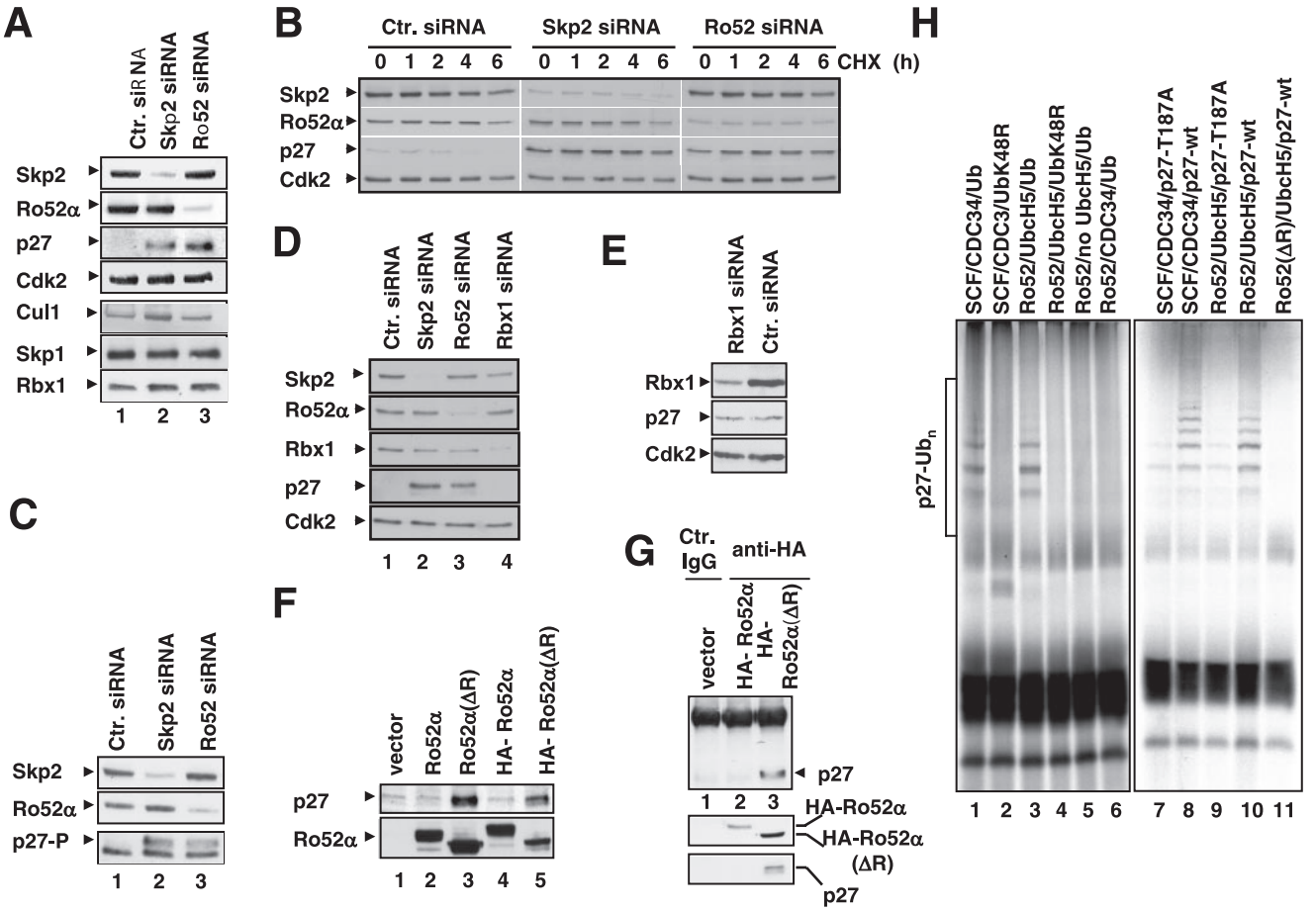

FIG. 5. Downregulation of Ro52 stabilizes p27. (A) HeLa cells were transfected with siRNAs corresponding to either nonrelevant mRNA (control siRNA) (lane 1), Skp2 mRNA (lane 2), or Ro52 mRNA (lane 3) and processed for immunoblotting with antibodies against indicated proteins. (B) The silencing of Skp2 and Ro52 was performed as described for panel A, and then cycloheximide (CHX) was added for the indicated times and lysates were processed for immunoblotting with antibodies against indicated proteins. (C) HeLa cells were transfected with indicated siRNAs and analyzed by immunoblotting using antibodies against Skp2, Ro52, and the Thr187-phosphorylated form of p27. (D and E) HeLa cells were transfected with indicated siRNAs and processed for immunoblotting for the specified proteins. (F) HeLa cells were transfected with empty vector (lane 1) or expression plasmids encoding untagged Ro52α(wt) (lane 2), untagged Ro52α(ΔR) (lane 3), HA-Ro52α(wt) (lane 4), or HA-Ro52α(ΔR) (lane 5) and processed for immunoblotting for p27 and Ro52. (G) Aliquots of lysates of HeLa cells transfected either with empty vector (lane 1) or with vectors to produce HA-Ro52α(wt) (lane 2) or HA-Ro52α(ΔR) (lane 3) were either subjected to immunoprecipitation with control mouse IgG (lane 1) or anti-HA 12CA5 (lanes 2 and 3) antibody, followed by immunoblotting with rabbit anti-p27 antibody (upper panel), or directly processed for immunoblotting using anti-HA MAb HA11 (middle panel) or anti-p27 antibody (lower panel). (H) Autoradiograms of ^{35}S-labeled p27(wt) (lanes 1 through 6, 8, 10, and 11) or p27(T187A) (lanes 7 and 9) after in vitro ubiquitination by anti-HA 12CA5 immunoprecipitates derived from HeLa cells that were transfected to produce HA-Ro52α, MT-Skp2, and MT-Cul1 (labeled with Ro52) or SCF^{Skp2} assembled in Sf9 cells (labeled with SCF). ctr., control.

grades Thr187-phosphorylated p27 in vivo. In stark contrast, p27 protein levels did not increase after the silencing of the RING finger protein Rbx1 with different siRNAs (Fig. 5D and E). Consistent with this, we did not observe a G_1-phase block in Rbx1 knockdown cells (data not shown). Thus, p27 degradation may depend, at least in this experimental system, primarily on Ro52 and not Rbx1. In further support for a key role of Ro52 in the abundance control of p27 in vivo, we found that enforced expression of either HA-tagged or untagged versions of Ro52α(ΔR), a mutant lacking the RING finger domain but able to interact with Skp2 and Cul1, resulted in a marked increase in the steady-state amounts of endogenous p27 (Fig. 5F, upper panel, lanes 3 and 5). Wild-type Ro52α was inactive in this regard (Fig. 5F, upper panel, lanes 2 and 4), although it was expressed in amounts similar to those of the mutant species (Fig. 5F, lower panel, lanes 2 and 4). Finally, we found that endogenous p27 coimmunoprecipitated efficiently with the transfected mutant species Ro52α(ΔR) (Fig. 5G), which is consistent with the view that this protein species may behave as a dominant negative insofar as it can bind Skp2 and Cul1 and capture p27 but fails to promote the degradation of the bound substrate due to the absence of the RING domain.

To directly examine whether Ro52α-containing complexes can promote p27 ubiquitination in vitro, we transfected HeLa cells with a combination of expression plasmids for HA-Ro52α, MT-Skp2, and MT-Cul1, lysed them, and used anti-HA immunoprecipitates as a source of E3 ligase. Immunoblotting experiments with anti-HA immunoprecipitates of such transfected cells revealed the presence of both MT-Skp2 and MT-Cul1 (data not shown). These Ro52α-containing complexes were

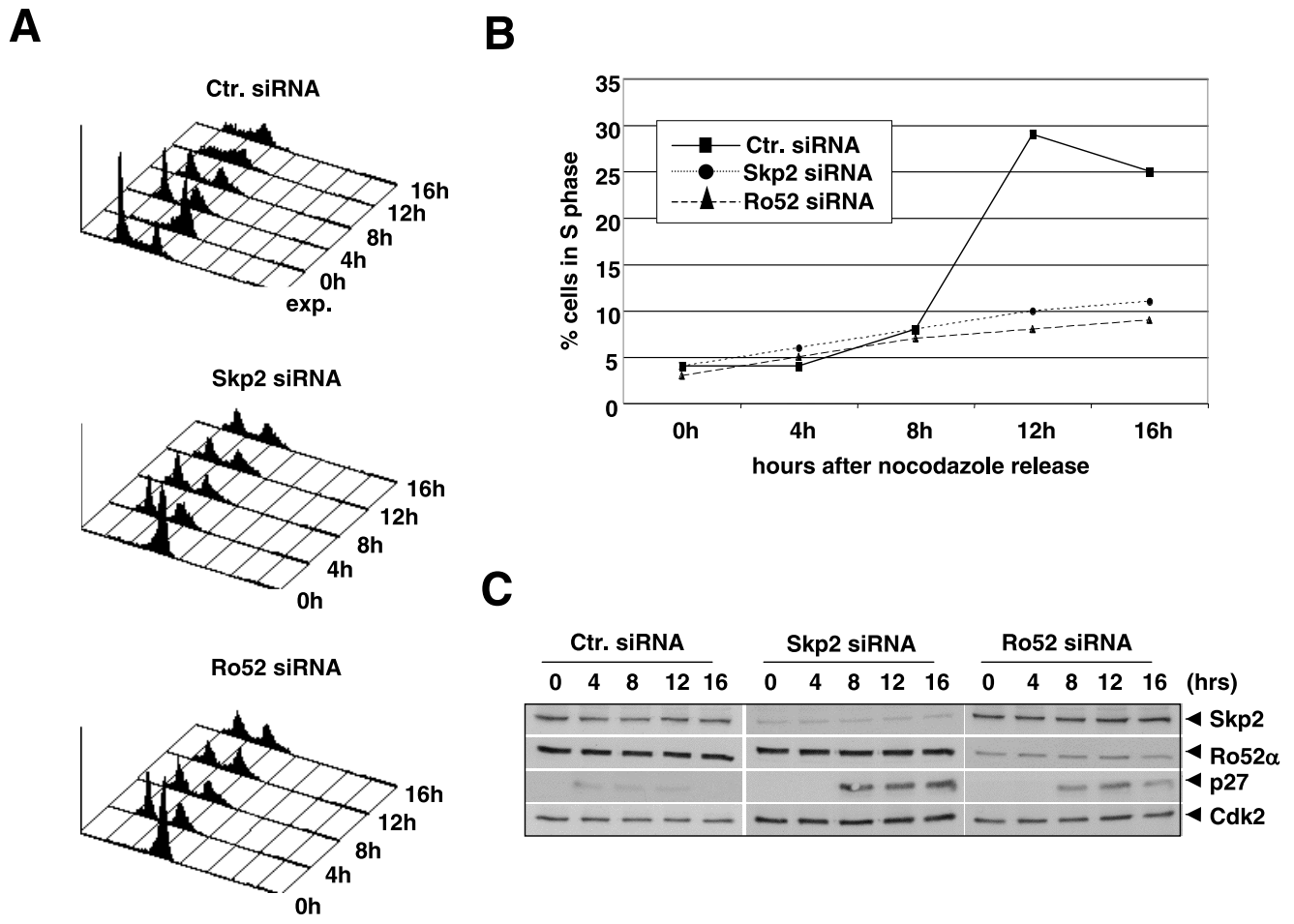

FIG. 6. Ro52 is required for S-phase progression. (A) Aliquots of HeLa cells transfected with the indicated siRNAs, synchronized by growth in nocodazole, and then released for the indicated periods of time were analyzed by FACS. The *y* axis indicates cell number and the *x* axis indicates DNA content as determined by propidium iodide staining. Exp., exponentially growing HeLa cells. (B) Percentage of cells in S phase analyzed as described for panel A. (C) Aliquots of cells shown in panel A were processed for immunoblotting with antibodies against indicated proteins. ctr., control.

incubated with [^{35}S]methionine-labeled p27(wt) substrate [which was previously phosphorylated by cyclin E-Cdk2 to provide the required Thr187 phosphorylation on p27(wt) for recognition by Skp2]. In the presence of ubiquitin, E1, and UbcH5, high-molecular-weight bands were formed (Fig. 5H, lane 3). These high-molecular-weight forms were similar to those generated by the classical SCF^{Skp2} assemblage in conjunction with the E2 enzyme CDC34 (lane 1). These high-molecular-weight bands failed to develop when ubiquitin was replaced by the mutant ubiquitin that inhibits ubiquitin chain elongation, ubiquitin(K48R) (lanes 2 and 4). The omission of UbcH5 or performing the ubiquitination reaction with the E2 enzyme CDC34 abolished the formation of a ubiquitin ladder by Ro52α-containing complexes (lanes 5 and 6, respectively). Consistent with the observation that siRNA-mediated down-regulation of Ro52 caused the accumulation of the Thr187-phosphorylated form of p27 in vivo (see Fig. 3B), Ro52 immune complexes, like SCF^{Skp2}, failed to promote the ubiquitination of p27(T187A) mutant protein, despite the presence of cyclin E-Cdk2 in these assays (Fig. 5H, lanes 9 and 7, respectively). Finally, Ro52-containing complexes formed with the RING finger-defective mutant Ro52α(ΔR) were inactive in mediating ubiquitination of p27(wt) (lane 11) and so were anti-HA immune complexes derived from transfections where either HA-Ro52α, MT-Skp2, or MT-Cul1 expression plasmids were omitted (data not shown). Moreover, we failed, thus far, to detect p27-directed E3 activity associated with Ro52-Cul1-Skp2-Skp1 complexes isolated from insect cells (data not shown), suggesting that additional subunits/post-translational modifications are required for Ro52-associated p27 ubiquitination activity. Taken together, these results imply that Ro52α RING finger protein complexes display E3 ubiquitination activity for Thr187-phosphorylated p27 in vitro.

Ro52 function is required for S-phase progression in mammalian cells. Since Skp2 function has been shown to be required for S-phase entry (33), we asked next whether Ro52 function would likewise be required for this process. To test this directly, HeLa cells were treated with either Skp2, Ro52,

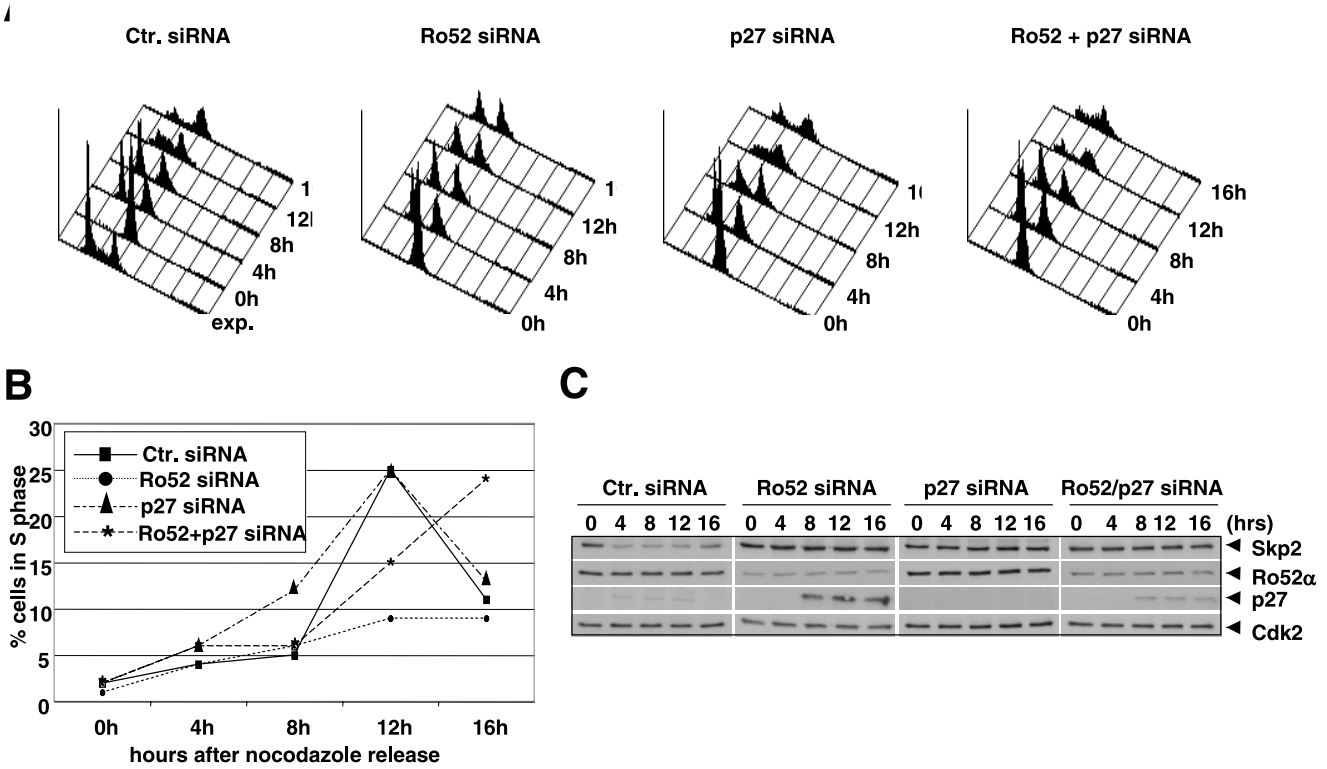

FIG. 7. Requirement for Ro52-mediated degradation of p27 for S-phase progression. (A) Aliquots of HeLa cells transfected with the indicated siRNAs were processed as described in the legend for Fig. 4A and analyzed by FACS. (B) Percentage of cells in S phase analyzed as described for panel A. (C) Aliquots of cells shown in panel A were processed for immunoblotting with antibodies against indicated proteins. ctr., control.

or control siRNAs, synchronized at mitosis with nocodazole, and released from the block. At various times thereafter, we monitored the cell cycle state by FACS and by immunoblotting for cell cycle markers. HeLa cells treated with control siRNA exited M phase and began to enter S phase approximately 10 to 12 h after release from the nocodazole block and continued to progress further into G_2 phase 4 h thereafter (Fig. 6A and B). Skp2-depleted cells also progressed into G_1 phase but failed to enter S phase (Fig. 6A and B), which was consistent with earlier reports (1, 35). Strikingly, siRNA-mediated Ro52 deficiency caused a similar block to S-phase entry (Fig. 6A and B). Concomitant with a failure of Skp2- or Ro52-deficient cells to enter S phase, they accumulated high levels of p27 protein (Fig. 6C). These results strongly suggest that Ro52 is an important regulator of mammalian S-phase progression.

Ro52 promotes S phase by targeting p27 for degradation. Based on these data, the question arose of whether the requirement of Ro52 for S-phase entry is, at least in part, linked to its p27 control function. To this end, we depleted Ro52 and p27, individually or together, and asked whether the block to S-phase progression after Ro52 removal was abrogated by p27 siRNA. As shown in Fig. 7, Ro52-depleted cells failed to enter S phase following release from a nocodazole block (Fig. 7A and B) and accumulated high levels of p27 (Fig. 7C). Cells treated with p27 siRNA progressed slightly faster into S phase (Fig. 7A and B), which is consistent with the absence of detectable p27 protein (Fig. 7C). Importantly, however, the codepletion of p27 reversed in part the inhibitory effect caused by Ro52 removal, allowing such cells to progress into S phase and further into G_2 (Fig. 7A and B). In keeping with this, the accumulation of p27 was markedly, albeit not entirely, attenuated in these cells (Fig. 7C). These results identify p27 as a critical target of Ro52's S-phase-promoting function.

DISCUSSION

The results presented here identify the RBCC family member Ro52 as a novel interaction partner of Skp2, Skp1, and Cul1 in vivo and a key participant of the mammalian S-phase progression pathway. Ro52 interacts also with at least one other F-box protein, βTrCP2, and, to a much lesser extent, with βTrCP1, but not with the BC-box protein pVHL. In this regard, Ro52 bound selectively to Cul1 but not to Cul2 or Cul3. The mapping of a Ro52 interaction domain to Cul1 residues 452 to 603, the site of Rbx/Roc interaction, implies that Ro52 may serve a role similar to that of Rbx/Roc in an SCF-like E3 ligase complex. This interpretation is supported by the finding that Ro52-containing complexes display RING-dependent ubiquitination activity in vitro directed towards the Thr187-phosphorylated form of p27. Moreover, human cells treated with Ro52 siRNA stabilize Thr187-phosphorylated p27 in vivo and fail to progress through S phase. Taken together, these results suggest a key role for the RING finger protein Ro52 in the process of p27 turnover and S-phase progression in mammalian cells and as a defining component of a novel SCF-like ubiquitin ligase complex.

There is emerging evidence that F-box proteins can assemble with diverse RING finger proteins to form ubiquitin ligase complexes. For example, the F-box protein Sel10/Ago/Fbw7/hCdc4, which is thought to target cyclin E for ubiquitin-mediated degradation in the context of an SCF assemblage to control cell cycle progression (13, 22, 32), has been reported to also associate with the RING finger protein parkin. This parkin-containing complex appears to contribute to the regulation of cyclin E in postmitotic neurons (36). Likewise, an SCF-like complex in *Caenorhabditis elegans* can use the RING finger protein RPM-1 instead of Rbx1/Roc1 family members (16). Thus, there appears to be combinatorial complexity in the assembly of F-box protein–RING finger protein interactions, which would allow for distinct modes of actions and regulation of F-box-driven ubiquitination processes.

The structural basis for the various protein/protein contacts within the multiprotein complex involving Ro52, Skp2, Skp1, and Cul1 is not fully understood. However, it would appear that the cullin homology domain is essential for Ro52-Cul1 interactions. This highly conserved segment has been previously shown to be essential for Rbx/Roc RING protein binding (37). Thus, the molecular interactions governing Cul1-Ro52 complex formation appear to recapitulate the generic cullin-RING domain architecture. With respect to Skp2, our data indicate that it can bind Ro52 in a manner that is F-box independent but LRR dependent, implying that, at least in vitro, Skp2 has an intrinsic capacity to bind Ro52 in the absence of Skp1. However, Skp1 appears to contribute to Skp2-Ro52 complex formation in vivo (Fig. 3F). These results support the view that Skp2 binding to Ro52 is an intrinsic property of the F-box protein (although it is not clear whether it is direct or indirect) and that Skp1 would facilitate/enhance complex formation. Since the depletion of Cul1 failed to noticeably affect Skp2-Ro52 complex formation, one might argue that Ro52-Cul1 interaction can occur independently of Ro52-Skp2 interactions. Irrespectively, based on these results, it is conceivable to propose the existence of a distinct SCF^{Skp2} complex that is defined by the nature of the RING finger protein. We propose to designate this complex $SCF^{Skp2/Ro52}$ to distinguish it from the "classical" SCF^{Skp2} quaternary complex containing Rbx/Roc RING protein.

It is well established that the decision to enter S phase relies on a series of regulatory inputs, including diverse metabolic, stress, and environmental cues. Thus, SCF^{Skp2} and $SCF^{Skp2/Ro52}$ may coexist to control p27 abundance in response to distinct signaling pathways or act dependent on cell type and context. Alternatively, these distinct E3 ligases may target different sets of substrates for ubiquitination. That the depletion of Rbx1 had no appreciable effects on p27 protein levels would support a model that, at least in certain cell types, $SCF^{Skp2/Ro52}$ may be the principle E3 ligase for p27 during the S-phase progression pathway. In this regard, there is evidence to suggest that the nature of the RING finger protein in F-box protein-based E3s can contribute to substrate specificity. This conclusion is supported by a recent functional analysis of *Drosophila* Rbx/Roc family members (26). In the fly, the F-box protein Slimb interacts with all members of the Rbx/Roc RING finger protein family and is known to be required for both cubitus interruptus and Armadillo/b-catenin (Arm) proteolysis. However, Roc1a mutants hyperaccumulate cubitus interruptus but not Arm, arguing that Slimb collaborates with an as-yet-to-be-identified RING finger protein to control Arm degradation. Since Skp2 has been implicated in the degradation of a diverse array of regulatory proteins (36), one might envision that Ro52 may contribute, at least in part, to the substrate specificity of Skp2.

Finally, increased Skp2 levels have been linked to poor prognoses in human cancer patients and its overexpression leads to proliferation and transformation in vitro and tumor formation in vivo (2, 9, 15). It will certainly be interesting to determine, in the future, whether Ro52 is also a target of alterations in human cancer and whether it conspires with Skp2 in promoting cell transformation and oncogenesis.

ACKNOWLEDGMENTS

We thank members of our laboratory for helpful discussions and advice, C. Frei and R. Ricci for critical reading of the manuscript, G. F. Draetta for the FT-βTrCP1/2 plasmids, H. Boeuf for the FT-mPIAS3L construct, and E. K. L. Chan for providing Ro52 cDNA.

This work was supported by the Novartis Research Foundation and a Collaborative Cancer Research Project grant from Oncosuisse and by grants from the European Community (U2P2) and the Swiss Cancer League to W.K.

REFERENCES

1. **Bashir, T., N. V. Dorrello, V. Amador, D. Guardavaccaro, and M. Pagano.** 2004. Control of the SCF(Skp2-Cks1) ubiquitin ligase by the APC/C(Cdh1) ubiquitin ligase. Nature **428:**190–193.
2. **Bloom, J., and M. Pagano.** 2003. Deregulated degradation of the cdk inhibitor p27 and malignant transformation. Semin. Cancer Biol. **13:**41–47.
3. **Carrano, A., E. Eytan, A. Hershko, and M. Pagano.** 1999. SKP2 is required for ubiquitin-mediated degradation of the CDK inhibitor p27. Nat. Cell Biol. **1:**193–199.
4. **Chan, E. K., F. Di Donato, J. C. Hamel, C. E. Tseng, and J. P. Buyon.** 1995. 52-kD SS-A/Ro: genomic structure and identification of an alternatively spliced transcript encoding a novel leucine zipper-minus autoantigen expressed in fetal and adult heart. J. Exp. Med. **182:**983–992.
5. **Chan, E. K., J. C. Hamel, J. P. Buyon, and E. M. Tan.** 1991. Molecular definition and sequence motifs of the 52-kD component of human SS-A/Ro autoantigen. J. Clin. Investig. **87:**68–76.
6. **Freemont, P. S.** 2000. RING for destruction? Curr. Biol. **10:**R84–R87.
7. **Fukuda-Kamitani, T., and T. Kamitani.** 2002. Ubiquitination of Ro52 autoantigen. Biochem. Biophys. Res. Commun. **295:**774–778.
8. **Ganoth, D., G. Bornstein, T. K. Ko, B. Larsen, M. Tyers, M. Pagano, and A. Hershko.** 2001. The cell-cycle regulatory protein Cks1 is required for SCF-(Skp2)-mediated ubiquitinylation of p27. Nat. Cell Biol. **3:**321–324.
9. **Gstaiger, M., R. Jordan, M. Lim, C. Catzavelos, J. Mestan, J. Slingerland, and W. Krek.** 2001. Skp2 is oncogenic and overexpressed in human cancers. Proc. Natl. Acad. Sci. USA **98:**5043–5048.
10. **Gstaiger, M., B. Luke, D. Hess, E. J. Oakeley, C. Wirbelauer, M. Blondel, M. Vigneron, M. Peter, and W. Krek.** 2003. Control of nutrient-sensitive transcription programs by the unconventional prefoldin URI. Science **302:**1208–1212.
11. **Hengstermann, A., L. K. Linares, A. Ciechanover, N. J. Whitaker, and M. Scheffner.** 2001. Complete switch from Mdm2 to human papillomavirus E6-mediated degradation of p53 in cervical cancer cells. Proc. Natl. Acad. Sci. USA **98:**1218–1223.
12. **Ishii, T., K. Ohnuma, A. Murakami, N. Takasawa, T. Yamochi, S. Iwata, M. Uchiyama, N. H. Dang, H. Tanaka, and C. Morimoto.** 2003. SS-A/Ro52, an autoantigen involved in CD28-mediated IL-2 production. J. Immunol. **170:**3653–3661.
13. **Koepp, D. M., L. K. Schaefer, X. Ye, K. Keyomarsi, C. Chu, J. W. Harper, and S. J. Elledge.** 2001. Phosphorylation-dependent ubiquitination of cyclin E by the SCFFbw7 ubiquitin ligase. Science **294:**173–177.
14. **Kossatz, U., N. Dietrich, L. Zender, J. Buer, M. P. Manns, and N. P. Malek.** 2004. Skp2-dependent degradation of p27kip1 is essential for cell cycle progression. Genes Dev. **18:**2602–2607.
15. **Latres, E., R. Chiarle, B. A. Schulman, N. P. Pavletich, A. Pellicer, G. Inghirami, and M. Pagano.** 2001. Role of the F-box protein Skp2 in lymphomagenesis. Proc. Natl. Acad. Sci. USA **98:**2515–2520.
16. **Liao, E. H., W. Hung, B. Abrams, and M. Zhen.** 2004. An SCF-like ubiquitin ligase complex that controls presynaptic differentiation. Nature **430:**345–350.
17. **Lisztwan, J., G. Imbert, C. Wirbelauer, M. Gstaiger, and W. Krek.** 1999. The von Hippel-Lindau tumor suppressor protein is a component of an E3 ubiquitin-protein ligase activity. Genes Dev. **13:**1822–1833.
18. **Lisztwan, J., A. Marti, H. Sutterluty, M. Gstaiger, C. Wirbelauer, and W.**

Krek. 1998. Association of human CUL-1 and ubiquitin-conjugating enzyme CDC34 with the F-box protein p45(SKP2): evidence for evolutionary conservation in the subunit composition of the CDC34-SCF pathway. EMBO J. **17:**368–383.

19. **Lorick, K. L., J. P. Jensen, S. Fang, A. M. Ong, S. Hatakeyama, and A. M. Weissman.** 1999. RING fingers mediate ubiquitin-conjugating enzyme (E2)-dependent ubiquitination. Proc. Natl. Acad. Sci. USA **96:**11364–11369.
20. **Marti, A., C. Wirbelauer, M. Scheffner, and W. Krek.** 1999. Interaction between ubiquitin-protein ligase SCFSKP2 and E2F-1 underlies the regulation of E2F-1 degradation. Nat. Cell Biol. **1:**14–19.
21. **Massague, J.** 2004. G1 cell-cycle control and cancer. Nature **432:**298–306.
22. **Moberg, K. H., D. W. Bell, D. C. Wahrer, D. A. Haber, and I. K. Hariharan.** 2001. Archipelago regulates cyclin E levels in Drosophila and is mutated in human cancer cell lines. Nature **413:**311–316.
23. **Montagnoli, A., F. Fiore, E. Eytan, A. C. Carrano, G. F. Draetta, A. Hershko, and M. Pagano.** 1999. Ubiquitination of p27 is regulated by Cdk-dependent phosphorylation and trimeric complex formation. Genes Dev. **13:**1181–1189.
24. **Nakayama, K., H. Nagahama, Y. A. Minamishima, M. Matsumoto, I. Nakamichi, K. Kitagawa, M. Shirane, R. Tsunematsu, T. Tsukiyama, N. Ishida, M. Kitagawa, K. Nakayama, and S. Hatakeyama.** 2000. Targeted disruption of Skp2 results in accumulation of cyclin E and p27Kip1, polyploidy and centrosome overduplication. EMBO J. **19:**2069–2081.
25. **Nakayama, K., H. Nagahama, Y. A. Minamishima, S. Miyake, N. Ishida, S. Hatakeyama, M. Kitagawa, S. Iemura, T. Natsume, and K. I. Nakayama.** 2004. Skp2-mediated degradation of p27 regulates progression into mitosis. Dev. Cell **6:**661–672.
26. **Noureddine, M. A., T. D. Donaldson, S. A. Thacker, and R. J. Duronio.** 2002. Drosophila Roc1a encodes a RING-H2 protein with a unique function in processing the Hh signal transducer Ci by the SCF E3 ubiquitin ligase. Dev. Cell **2:**757–770.
27. **Reymond, A., G. Meroni, A. Fantozzi, G. Merla, S. Cairo, L. Luzi, D. Riganelli, E. Zanaria, S. Messali, S. Cainarca, A. Guffanti, S. Minucci, P. G. Pelicci, and A. Ballabio.** 2001. The tripartite motif family identifies cell compartments. EMBO J. **20:**2140–2151.
28. **Rhodes, D. A., G. Ihrke, A. T. Reinicke, G. Malcherek, M. Towey, D. A. Isenberg, and J. Trowsdale.** 2002. The 52 000 MW Ro/SS-A autoantigen in Sjögren's syndrome/systemic lupus erythematosus (Ro52) is an interferon-gamma inducible tripartite motif protein associated with membrane proximal structures. Immunology **106:**246–256.
29. **Scheffner, M., J. M. Huibregtse, and P. M. Howley.** 1994. Identification of a human ubiquitin-conjugating enzyme that mediates the E6-AP-dependent ubiquitination of p53. Proc. Natl. Acad. Sci. USA **91:**8797–8801.
30. **Sherr, C. J., and J. M. Roberts.** 1999. CDK inhibitors: positive and negative regulators of G1-phase progression. Genes Dev. **13:**1501–1512.
31. **Spruck, C., H. Strohmaier, M. Watson, A. P. Smith, A. Ryan, T. W. Krek, and S. I. Reed.** 2001. A CDK-independent function of mammalian Cks1: targeting of SCF(Skp2) to the CDK inhibitor p27Kip1. Mol. Cell **7:**639–650.
32. **Strohmaier, H., C. H. Spruck, P. Kaiser, K. A. Won, O. Sangfelt, and S. I. Reed.** 2001. Human F-box protein hCdc4 targets cyclin E for proteolysis and is mutated in a breast cancer cell line. Nature **413:**316–322.
33. **Sutterluty, H., E. Chatelain, A. Marti, C. Wirbelauer, M. Senften, U. Muller, and W. Krek.** 1999. p45SKP2 promotes p27Kip1 degradation and induces S phase in quiescent cells. Nat. Cell Biol. **1:**207–214.
34. **Tsvetkov, L. M., K. H. Yeh, S. H. Lee, H. Sun, and H. Zhang.** 1999. p27 ubiquitination and degradation is regulated by the SCFSkp2 complex through phosphorylated thr 187 in p27. Curr. Biol. **9:**661–664.
35. **Wei, W., N. G. Ayad, Y. Wan, G. J. Zhang, M. W. Kirschner, and W. G. Kaelin, Jr.** 2004. Degradation of the SCF component Skp2 in cell-cycle phase G1 by the anaphase-promoting complex. Nature **428:**194–198.
36. **Willems, A. R., M. Schwab, and M. Tyers.** 2004. A hitchhiker's guide to the cullin ubiquitin ligases: SCF and its kin. Biochim. Biophys. Acta **1695:**133–170.
37. **Wirbelauer, C., H. Sutterluty, M. Blondel, M. Gstaiger, M. Peter, F. Reymond, and W. Krek.** 2000. The F-box protein Skp2 is a ubiquitylation target of a Cul1-based core ubiquitin ligase complex: evidence for a role of Cul1 in the suppression of Skp2 expression in quiescent fibroblasts. EMBO J. **19:**5362–5375.